



Effects of Pb and Mg doping in Al₂O₃-supported Pd catalyst on direct oxidative esterification of aldehydes with alcohols to esters

Yanyan Diao^{a,b}, Ruiyi Yan^{a,b}, Suojiang Zhang^{a,*}, Pu Yang^a, Zengxi Li^b, Lei Wang^a, Haifeng Dong^{a,b}

^a Key Laboratory of Green Process and Engineering, Institute of Process Engineering, Chinese Academy of Sciences, 100190 Beijing, China

^b Graduate University of Chinese Academy of Sciences, 100049 Beijing, China

ARTICLE INFO

Article history:

Received 17 May 2008

Received in revised form 11 December 2008

Accepted 28 December 2008

Available online 8 January 2009

Keywords:

Oxidative esterification

Pd catalyst

Pb doping

Mg doping

Pb and Mg doping

ABSTRACT

An investigation was carried out of oxidative esterification of aldehydes with alcohols and oxygen to corresponding esters over Pb, Mg-doped Al₂O₃-supported Pd catalyst. This catalyst was prepared by impregnating method and characterized by X-ray diffraction, differential scanning calorimetry, X-ray photoelectron spectroscopy, and transmission electron microscopy. The results showed that Pd atoms with Pb atoms formed bimetallic Pd₃Pb crystals, and Mg existed on the support as MgO with electron effect on Pd₃Pb crystals. The reactions of aldehyde with alcohol in the presence and absence of oxygen over the doped and undoped Pd catalysts were examined to evaluate the effects of Pb and Mg. It was found that the doping agents Mg had positive effect on reaction rate acceleration only in the presence of oxygen, Pb or the collaboration of Pb and Mg had positive effect on reaction rate acceleration and selectivity enhancement in the presence of oxygen or not.

© 2009 Elsevier B.V. All rights reserved.

1. Introduction

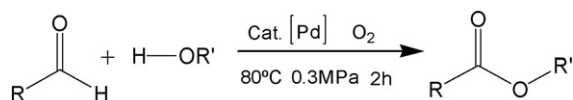
Direct oxidative esterification of aldehydes with alcohols to corresponding esters under mild conditions is a useful reaction in organic synthesis and industrialization; hence, much effort has been devoted to find newer methods and newer reagents effective for this type of reaction. So far, this process of oxidative esterification has been accomplished in a variety of ways. Two-step methods include oxidation of acetals [1], cyanohydrins [2], etc. One-step conventional methods reported require the use of heavy-metal oxidants such as KMnO₄ [3], CrO₃ [4]. Electrochemical oxidation [5], as well as very recently using catalyst V₂O₅/H₂O₂ [6] and catalyst [IrCl(cod)]₂/K₂CO₃ [7], also have been reported. Most of reported methods are useful for direct transformation of aldehydes with alcohols to corresponding esters. However, many methods suffer from disadvantages such as use of an amount of expensive and polluting reagents, an inert atmosphere, lengthy reaction times, and electrochemical conditions. Some of these reagents are also unsatisfactory for specific transformation of aldehydes containing deactivated, hindered, and double-bond-containing substrates, resulting in undesirable products. The authors have therefore sought to develop a catalytic route with respect to environmentally benign catalyst and reagent, cost-effectiveness, mild reaction condition, shorter reaction time, and facile isolation of required

product. Now method for the oxidative esterification of aldehydes with alcohols and oxygen to corresponding esters using the Pb, Mg-doped Al₂O₃-supported Pd as catalyst, O₂ or air as oxidant is presented in this paper (Scheme 1). This oxidant is atom efficient and produces water as only by-product.

It is known that metallic Pd catalysts are often used for selective oxidation or oxygenation reaction [8–13], and Pb and Bi display attractive properties as doping elements in noble metal-based catalysts. It has been reported that the doping agents of bimetallic supported catalysts can prevent the leaching of noble metal [14,15]. In addition, the doped metals alone are inactive in oxidation under the mild conditions applied; still, they can sometimes induce spectacular rate enhancement or a shift in the product distribution [16–20]. Several strategies have been applied to understand the effects of doping agents of bi- and trimetallic catalysts, including the synthesis and catalytic test of intermetallic compounds [21], in situ study of the oxidation state of the metals by electrochemical methods [22,23] and X-ray absorption spectroscopy (XAS) [24,25], and the detailed kinetic analysis of the reaction [26]. However, the real nature of the doping agent on oxidation is still debated. Accordingly, the effects of doping agents Pb and Mg on direct oxidative esterification are also not understood. It is not clearly established that whether the doping agents Pb and Mg play a role in the catalytic process or if they merely modify the supported nano-Pd catalyst.

In this paper, in order to study the structure of Pb, Mg-doped Al₂O₃-supported Pd catalyst and the existing state of these doping agent Pb and Mg, the doped and undoped Pd catalysts were extensively characterized by X-ray diffraction (XRD), differential

* Corresponding author. Tel.: +86 10 8262 7080; fax: +86 10 8262 7080.
E-mail address: gct@home.ipe.ac.cn (S. Zhang).



Scheme 1. Pd-catalyzed oxidative esterification of aldehydes with alcohols to corresponding esters.

scanning calorimetry (DSC), X-ray photoelectron spectroscopy (XPS), and transmission electron microscopy (TEM). Moreover, a wide range of aldehydes and alcohols were chosen to examine the activity and selectivity of Pb, Mg-doped Al_2O_3 -supported Pd catalyst for oxidative esterification of aldehydes with alcohols and oxygen to corresponding esters. In order to examine the effects of Pb and Mg on direct oxidative esterification, methacrolein and methanol were chosen as test substrates to react in different reaction atmospheres over doped and undoped Pd catalysts. In addition, to improve the understanding of their effects, more attention was paid to the individual effect of doping agents.

2. Experimental

2.1. Preparation of supported Pd catalysts

The catalysts used in experiments with the compositions expressed as 5 wt.% Pd/ Al_2O_3 , 5 wt.% Pd–2 wt.% Mg/ Al_2O_3 , 5 wt.% Pd–5 wt.% Pb/ Al_2O_3 and 5 wt.% Pd–5 wt.% Pb–2 wt.% Mg/ Al_2O_3 , which were abbreviated as Pd₅/ Al_2O_3 , Pd₅Mg₂/ Al_2O_3 , Pd₅Pb₅/ Al_2O_3 and Pd₅Pb₅Mg₂/ Al_2O_3 , were prepared according to the following procedure. An aqueous magnesium acetate solution was heated to the temperature of 50–100 °C under stirring, then an appropriate amount of the support $\gamma\text{-Al}_2\text{O}_3$ (200–250 μm) was added to this magnesium acetate impregnating liquid. Until water was evaporated, the obtained support Al_2O_3 adsorbing all amounts of magnesium acetate was dried under vacuum at 45 °C for 12 h, and then calcined at 600 °C in air for 3 h. Mg-doped Al_2O_3 that abbreviated as Mg₂/ Al_2O_3 was obtained. An appropriate amount of $\gamma\text{-Al}_2\text{O}_3$ or Mg₂/ Al_2O_3 was impregnated by an aqueous palladium chloride solution at 50–100 °C under stirring for 1 h, and then was reduced by an aqueous hydrazine solution for 3 h. The support on which palladium had been adsorbed and reduced was filtered and washed with distilled water several times, then dried under vacuum at 45 °C for 12 h. Catalysts Pd₅/ Al_2O_3 and Pd₅Mg₂/ Al_2O_3 were obtained. The impregnating liquid of aqueous palladium chloride solution was replaced by the aqueous palladium chloride and lead acetate mixed solution according to the procedure described above, catalysts Pd₅Pb₅/ Al_2O_3 and Pd₅Pb₅Mg₂/ Al_2O_3 were obtained.

The catalysts Pd₅/ Al_2O_3 , Pd₅Mg₂/ Al_2O_3 , Pd₅Pb₅/ Al_2O_3 , and Pd₅Pb₅Mg₂/ Al_2O_3 were all kept in a vacuum oven before being used.

2.2. Characterization

Several characterization techniques were applied to characterize the supported Pd catalysts in this work. The actual contents of Pd, Pb and Mg in the catalysts were all determined by using OPTIMA 5300DV inductively coupled plasma-mass emission spectrometry (ICP-MS) manufactured by PerkinElmer. The known weight of the catalyst was dissolved in the mixture of hydrochloric acid (HCl) and nitric acid (HNO₃) with volume proportion as 3:1. The solution obtained after complete dissolution was diluted to required volume. The samples were analyzed to determine Pd, Pb and Mg contents. XRD patterns were obtained with X'Pert Pro MPD X-ray diffractometer from PANalytical, using Cu K α radiation ($\lambda = 0.154187$ nm) and scanning angle 2θ from 10° to 90°.

DSC experiments were performed using a conventional differential scanning calorimeter (NETZSCH STA 449C), which is connected

to a thermal analysis operation system. For the ambient pressure DSC analysis, about 8 mg of a sample was weighed. The sample was heated from room temperature to 500 °C at a heating rate of 20 °C/min in air flow of 60 mL/min. XPS data were obtained with an ESCALab220i-XL electron spectrometer from VG Scientific using 300 W Al K α radiations. The base pressure was about 3×10^{-9} mbar. The binding energies were referenced to C 1s line at 284.8 eV from adventitious carbon. TEM analysis was performed using an FEI Tecnai 20 electronic microscope. The specimens for TEM analysis were prepared by dispersing the products in ethanol followed by ultrasonic treatment. The samples were then deposited onto a holey carbon film supported on a copper grid and dried in air.

2.3. Catalytic transformation of aldehydes with alcohols to corresponding esters

Catalytic reactions were carried out by a bench-scale. 2.0 g prepared catalyst (catalyst Pd₅/ Al_2O_3 , Pd₅Mg₂/ Al_2O_3 , Pd₅Pb₅/ Al_2O_3 or Pd₅Pb₅Mg₂/ Al_2O_3), 0.3 mol aldehyde, and 1.5 mol alcohol were added into a flat-bottomed, magnetically stirred 100-mL stainless steel reactor. In addition, 1.0 mL 2 wt.% solution of NaOH in corresponding alcohol and 0.1 g Mg(OH)₂ were also added into the reactor to neutralize the produced carboxylic acid and keep the solution pH at a value of 6.0–8.0. Reactions were carried out under 80 °C and pressure of 3 kg/cm². The O₂ (or He) flow rate of 30 mL/min and constant stirring speed of 1 000 r/min were set to ensure the reactions in mass-transport-limited regime and avoid over-oxidation of the catalyst [14,27]. The reactions were stopped after 2 h. The reaction mixtures were analyzed by GC (Agilent 6890, equipped with DB-624 capillary column and an FID detector). Products were identified by GC–MS.

Catalytic results were expressed as conversion rate (X, %) and selectivity (S, %) which were determined by GC using ethanol as external standard. Those parameters are defined as

$$X(\text{mol}\%) = \left(1 - \frac{C_{\text{aldehyde}}}{C_{0\text{aldehyde}}}\right) \times 100\%$$

$$S(\text{mol}\%) = \left(\frac{C_{\text{ester}}}{C_{0\text{aldehyde}} - C_{\text{aldehyde}}}\right) \times 100\%$$

where $C_{0\text{aldehyde}}$ is the molar concentration of aldehyde at the beginning of the direct transformation process, C_{aldehyde} the molar concentration of aldehyde after time t , and C_{ester} is the molar concentration of the corresponding ester after time t .

3. Results and discussion

3.1. Structure of Pb and Mg-doped Al_2O_3 -supported Pd catalyst

Table 1 gives the results of the ICP-MS measurements of the actual Pd, Pb and Mg amounts in the doped and undoped catalysts. The results of ICP-MS measurements are consistent with the results of the proposed method.

Fig. 1(a) shows XRD patterns of all samples, including the support Al_2O_3 , Mg₂/ Al_2O_3 , catalysts Pd₅/ Al_2O_3 , Pd₅Mg₂/ Al_2O_3 ,

Table 1
ICP measurements of actual Pd, Pb and Mg contents in the doped and undoped catalysts.

Catalyst	Pd (wt.%)	Pb (wt.%)	Mg (wt.%)
Pd ₅ / Al_2O_3	4.93	–	–
Pd ₅ Mg ₂ / Al_2O_3	4.96	–	1.95
Pd ₅ Pb ₅ / Al_2O_3	4.94	4.92	–
Pd ₅ Pb ₅ Mg ₂ / Al_2O_3	4.91	4.90	1.94

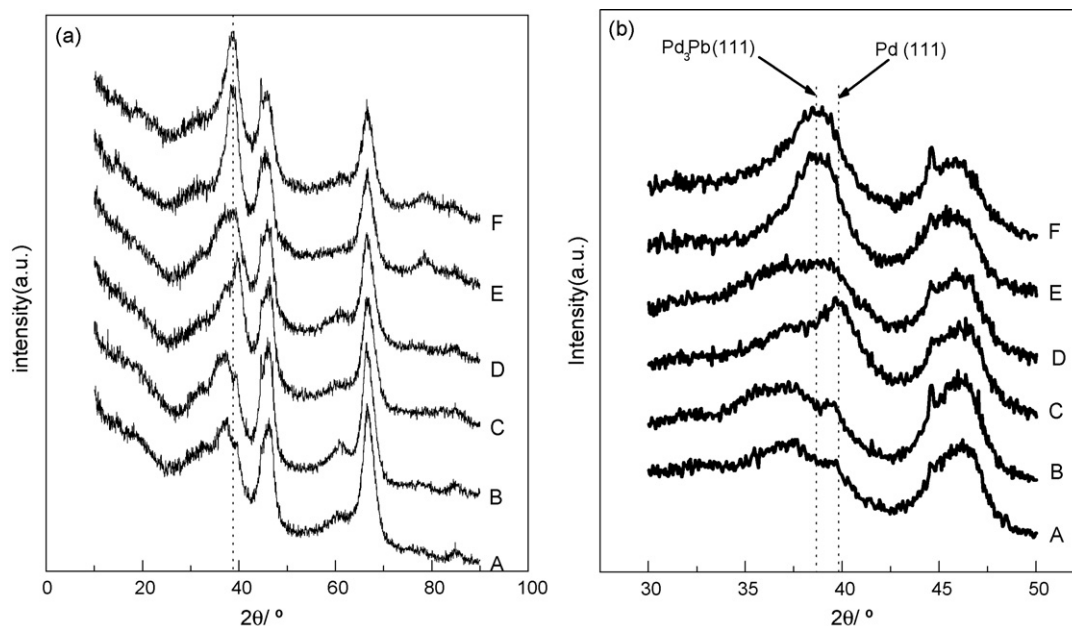


Fig. 1. XRD patterns of support Al_2O_3 (A), $\text{Mg}_2/\text{Al}_2\text{O}_3$ (B), catalysts $\text{Pd}_5/\text{Al}_2\text{O}_3$ (C), $\text{Pd}_5\text{Mg}_2/\text{Al}_2\text{O}_3$ (D), $\text{Pd}_5\text{Pb}_5/\text{Al}_2\text{O}_3$ (E) and $\text{Pd}_5\text{Pb}_5\text{Mg}_2/\text{Al}_2\text{O}_3$ (F). Full 2θ range shown in (a), with region of metallic Pd(1 1 1) reflections shown in more detail in (b).

$\text{Pd}_5\text{Pb}_5/\text{Al}_2\text{O}_3$ and $\text{Pd}_5\text{Pb}_5\text{Mg}_2/\text{Al}_2\text{O}_3$. No change of peaks of $\text{Mg}_2/\text{Al}_2\text{O}_3$ compared with these of Al_2O_3 indicated that the introduction of Mg atoms to Al_2O_3 had no influence on the structure of Al_2O_3 , and no new peak of $\text{Mg}_2/\text{Al}_2\text{O}_3$ indicated the wonderful dispersion of Mg on the support Al_2O_3 . In order to focus on Pd (1 1 1) reflection, the recorded 2θ range of Fig. 1(b) was from 30° to 50° . The new peaks of catalysts $\text{Pd}_5/\text{Al}_2\text{O}_3$ and $\text{Pd}_5\text{Mg}_2/\text{Al}_2\text{O}_3$ at about 39.7° were corresponding to d_{111} reflection of monometallic Pd crystals. The new peaks of catalysts $\text{Pd}_5\text{Pb}_5/\text{Al}_2\text{O}_3$ and $\text{Pd}_5\text{Pb}_5\text{Mg}_2/\text{Al}_2\text{O}_3$ at about 38.6° were corresponding to d_{111} reflection of bimetallic Pd_3Pb crystals, indicating that Pb atoms with Pd atoms formed alloy Pd_3Pb crystals with face-center cubic structure [28]. The width and intensity of peaks are the indication of the metal crystal size (the wider the diffraction peak, the less intense the peak, and the smaller the crystal size) [29]. For Mg-doped monometallic Pd and bimetallic Pd_3Pb crystal catalysts, there were a little decrease of the monometallic Pd (1 1 1) intensity and bimetallic Pd_3Pb (1 1 1) intensity (joining to a wider peak) compared with that of Mg-undoped catalysts. This result indicated that the monometallic Pd and bimetallic Pd_3Pb crystals on Mg-doped catalysts were a little smaller than that on Mg-undoped catalysts. The small crystals were supposed to increase the activity of catalyst [9].

DSC analysis was performed in the atmosphere of air, so the peaks showed in Fig. 2 represented the oxidative temperature of metals. There was no peak of the oxidation of metallic state Pb when only Pb was doped in Al_2O_3 (Fig. 2(a)). This observed result indicated that Pb existed on the support as Pb^{2+} when no metallic state Pd existed. The basic idea is that Pb^{2+} cannot be reduced to Pb^0 on the surface of the support Al_2O_3 under ambient conditions by an aqueous hydrazine solution, but it is readily reduced on the unsaturated Pd site to form metal atom. As discussed above, the reducible fractions of Pb atoms were located on bimetallic Pd_3Pb crystals, and results in Fig. 2(a) shows that the oxidation of Pd_3Pb crystals took place at much higher temperature than the oxidation of monometallic Pd crystals. Pd_3Pb crystals oxidation took place at around 605 K and in the case of monometallic Pd crystals at around 558 K. Fig. 2(a) also shows that no monometallic state Pd and monometallic state Pb existed on catalyst $\text{Pd}_5\text{Pd}_5/\text{Al}_2\text{O}_3$.

Fig. 2(b) shows that the oxidation (around 545 K) of monometallic Pd crystals on catalyst $\text{Pd}_5\text{Mg}_2/\text{Al}_2\text{O}_3$ took place at a little lower temperature than the oxidation (around 558 K) of monometallic Pd crystals on catalyst $\text{Pd}_5/\text{Al}_2\text{O}_3$. As discussed in XRD analysis, the monometallic Pd crystals on catalyst $\text{Pd}_5\text{Mg}_2/\text{Al}_2\text{O}_3$ were smaller than that on catalyst $\text{Pd}_5/\text{Al}_2\text{O}_3$. For catalysts $\text{Mg}_2/\text{Al}_2\text{O}_3$ and $\text{Pd}_5\text{Mg}_2/\text{Al}_2\text{O}_3$, no peaks of the oxidation of metallic state Mg indicated that Mg existed on the support as MgO , which made monometallic Pd and bimetallic Pd_3Pb crystals on the support a little small.

The surface compositions of catalysts $\text{Pd}_5/\text{Al}_2\text{O}_3$, $\text{Pd}_5\text{Pd}_5/\text{Al}_2\text{O}_3$ and $\text{Pd}_5\text{Pb}_5\text{Mg}_2/\text{Al}_2\text{O}_3$ were determined by XPS. Figs. 3 and 4 show strong modifications of the Pd 3d-band and Pb 4f-band. The 3d XPS spectra of Pd displayed two doublets which could be assigned to Pd^0 and Pd^{2+} (Fig. 3). The two doublets of Pb corresponded to Pb^0 and Pb^{2+} (Fig. 4). It was determined that certain amounts of Pd and Pb remained in the support–alumina interphase as Pd^{2+} and Pb^{2+} . As discussed in DSC analysis, no monometallic state Pd existed on Pb-doped Pd catalysts, so the reducible fraction of Pd was all located on bimetallic crystal Pd_3Pb , and the fractions of unreducible Pb and Pd corresponding to Pb^{2+} and Pd^{2+} species presented on alumina. In both cases, the majorities of Pd existed on the support as metallic state (Table 2). The fraction of unreducible Pd indicated that catalysts were not completely reduced. The fractions of unreducible Pb^{2+} and Pd^{2+} species presented on alumina were assumed ineffective in catalytic reaction. Thus, a well-prepared and reduced catalyst should contain only small amounts of Pb^{2+} and Pd^{2+} species on the support. More details of the analysis of Pd 3d and Pb 4f signals in these bimetallic catalysts can be found in Table 2. Pd^{2+} and Pb^{2+} species, being inactive for the reaction, will not be considered for the purpose of present study.

Table 2 shows Pd 3d and Pb 4f binding energy shifts and molar ratios of $\text{Pd}^0/(\text{Pd}^0 + \text{Pd}^{2+})$ and $\text{Pb}^0/(\text{Pb}^0 + \text{Pb}^{2+})$. From the peak top position, the binding energies of Pd $3d_{5/2}$ and $3d_{3/2}$ decreased when the doping agent of Pb was added to catalyst $\text{Pd}_5/\text{Al}_2\text{O}_3$. Therefore, electron transfer from Pb to Pd in bimetallic Pd_3Pb crystals was suggested. When the doping agent of Mg was added to catalyst $\text{Pd}_5\text{Pb}_5/\text{Al}_2\text{O}_3$, the binding energies of Pd $3d_{5/2}$ and $3d_{3/2}$ decreased, whereas the binding energies of Pb $4f_{7/2}$ and $4f_{5/2}$ did not change.

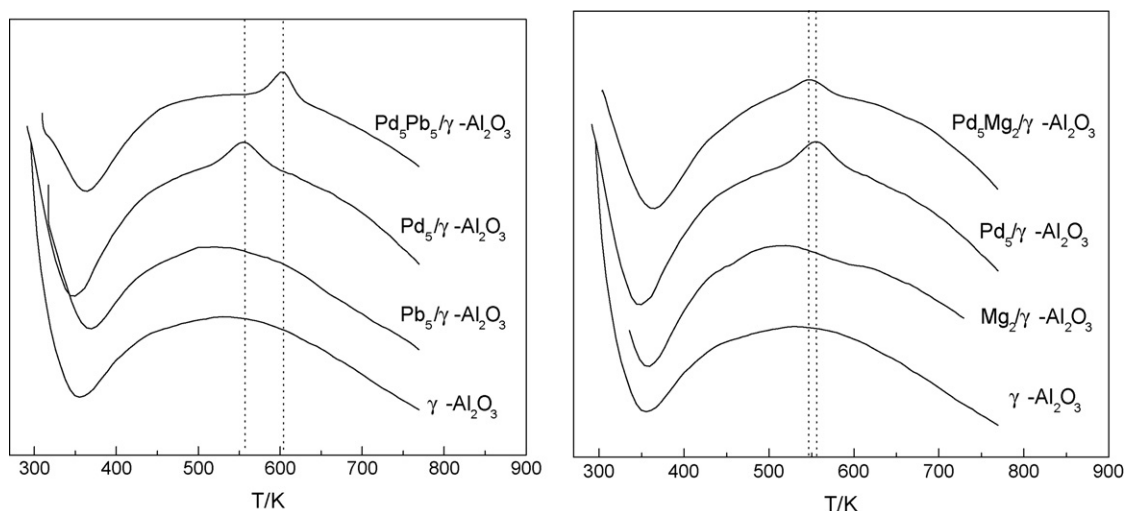


Fig. 2. DSC patterns of support and catalysts.

Thus, the decrease of binding energies of Pd $3d_{5/2}$ and $3d_{3/2}$ was attributed to the electron effect of Mg. As referred just above, this change of electron density of Pd would be related to adsorptive behavior.

The surface contents of Pb and Pd observed in these catalysts through XPS were systematically lower than that of theoretical values. The majorities of Pd were on the inner region of the catalyst not on the outer surface. The surface Pd content (1.38 wt.%) of Pb, Mg-doped Pd catalyst was lower than that (5.02 wt.%) of undoped

Pd catalyst. The analytical results indicated that low atomic intensity of noble metal Pd on the outer surface could prevent the much leaching of noble metal Pd.

The nano-particle sizes of Pd₃Pb crystals on catalysts Pd₅Pb₅/Al₂O₃ and Pd₅Pb₅Mg₂/Al₂O₃ were demonstrated by TEM images, as shown in Fig. 5. For determination of metal crystal size, different areas were examined and about 200 crystals counted. The mean diameter of bimetallic Pd₃Pb crystals on catalyst Pd₅Pb₅/Al₂O₃ was 4.7 nm and that on catalyst

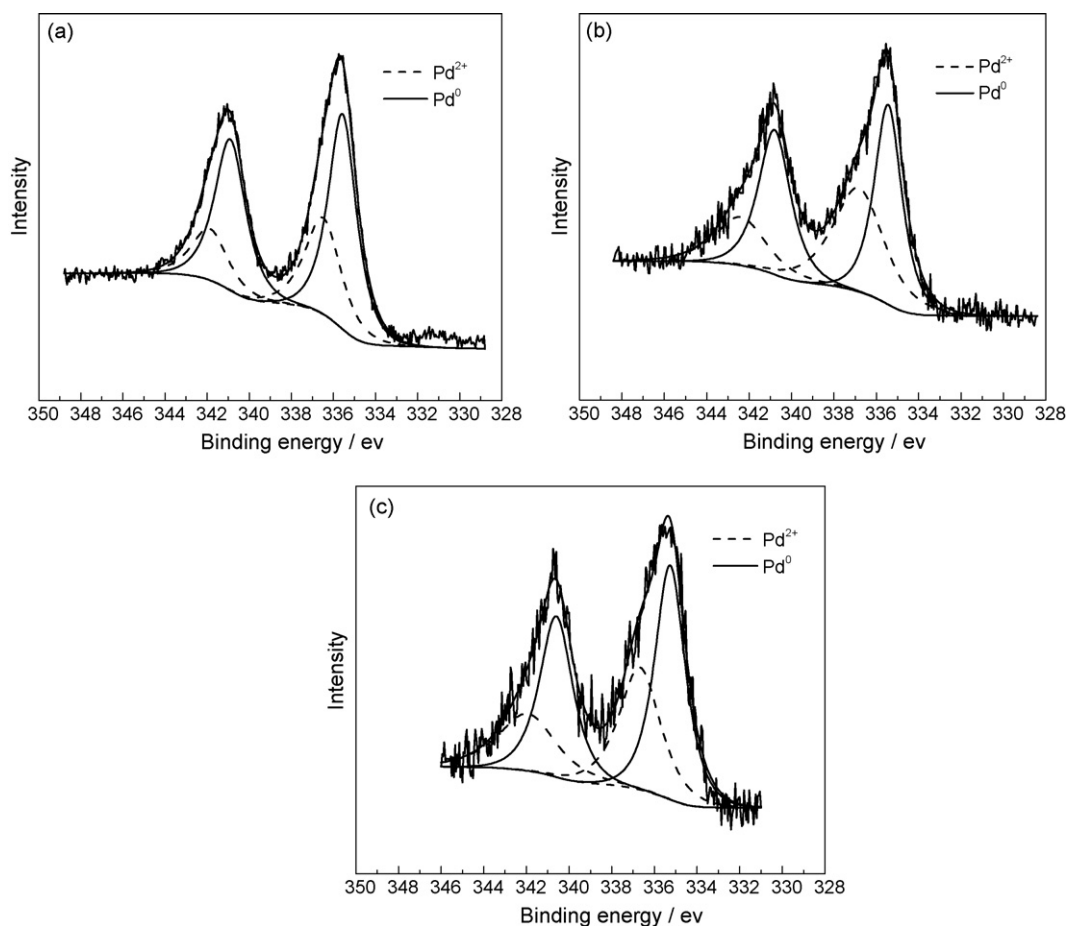


Fig. 3. Curve fittings of Pd $3d$ spectra of catalysts Pd₅/Al₂O₃ (a), Pd₅Pb₅/Al₂O₃ (b), and Pd₅Pb₅Mg₂/Al₂O₃ (c).

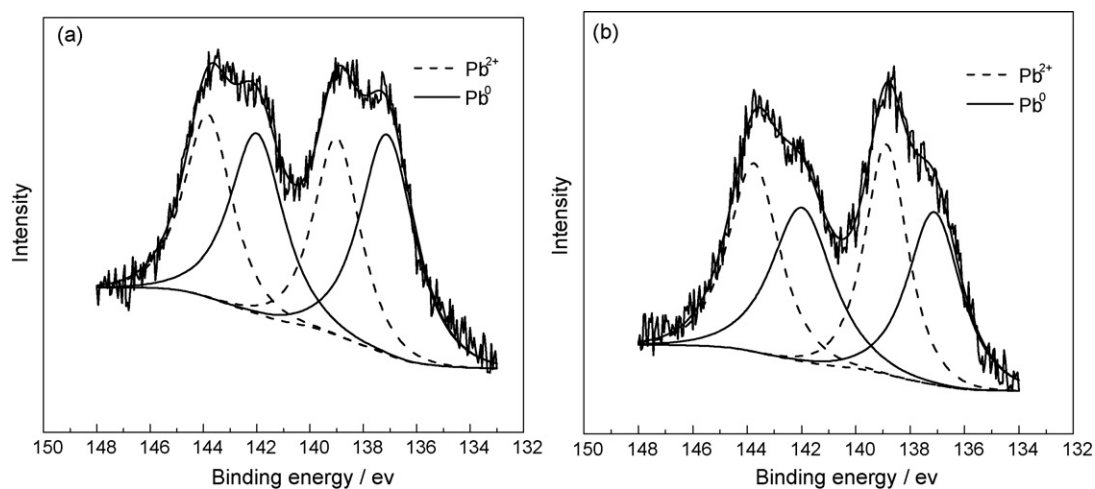


Fig. 4. Curve fittings of Pb 4f spectra of catalysts Pd₅Pb₅/Al₂O₃ (a) and Pd₅Pb₅Mg₂/Al₂O₃ (b).

Table 2

XPS analysis of Pd 3d-peaks and Pb 4f-peaks in the doped and undoped catalysts.

Catalyst	Binding energy and content	Pd ⁰		Pd ²⁺		Pb ⁰		Pb ²⁺	
		3d _{5/2}	3d _{3/2}	3d _{5/2}	3d _{3/2}	4f _{7/2}	4f _{5/2}	4f _{7/2}	4f _{5/2}
Pd ₅ /Al ₂ O ₃	Binding energy (eV)	335.6	340.9	336.5	341.8	–	–	–	–
	Content (%)	42.9	34.1	16.4	6.6	–	–	–	–
Pd ₅ Pb ₅ /Al ₂ O ₃	Binding energy (eV)	335.4	340.7	336.3	341.6	137.1	142.0	139.0	143.8
	Content (%)	35.8	31.0	24.5	8.7	25.6	19.5	28.0	26.9
Pd ₅ Pb ₅ Mg ₂ /Al ₂ O ₃	Binding energy (eV)	335.3	340.6	336.2	341.5	137.1	142.0	139.0	143.8
	Content (%)	39.3	30.7	19.1	10.9	24.4	21.8	29.8	25.0

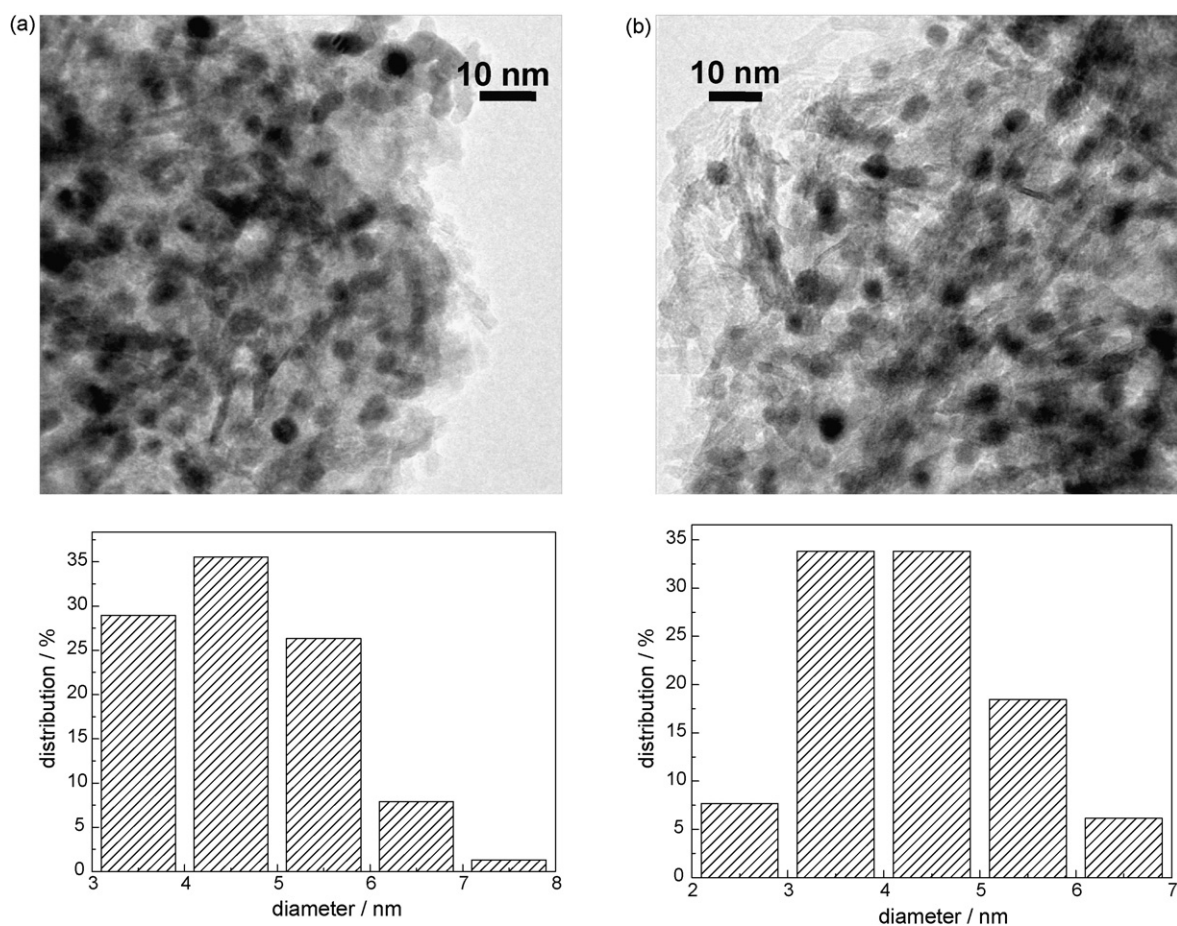


Fig. 5. TEM images and the size distributions of bimetallic Pd₃Pb crystals for catalysts Pd₅Pb₅/Al₂O₃ (a) and Pd₅Pb₅Mg₂/Al₂O₃ (b).

$\text{Pd}_5\text{Pb}_5\text{Mg}_2/\text{Al}_2\text{O}_3$ was 4.2 nm. Crystals in these catalysts had a uniform size. The uniform size distribution was supposed to have a good activity. It must be taken into account that the crystal size of monometallic Pd or bimetallic Pd_3Pb crystals depends on many factors such as the support, the noble metal precursor salt selected, and heating atmosphere, time and temperature [30]. Given that, initial preparation methods were the same, so the slightly smaller bimetallic crystals on catalyst $\text{Pd}_5\text{Pb}_5\text{Mg}_2/\text{Al}_2\text{O}_3$ than those on catalyst $\text{Pd}_5\text{Pb}_5/\text{Al}_2\text{O}_3$ were attributed to the effect of Mg.

3.2. Direct transformation of aldehydes with alcohols to corresponding esters

Under the reaction condition, a wide range of aldehydes including aromatic, aliphatic, and conjugated aldehydes with alcohols all could be converted to corresponding esters over catalyst $\text{Pd}_5\text{Pb}_5\text{Mg}_2/\text{Al}_2\text{O}_3$ in the atmosphere of oxygen. As seen from Table 3, most of aldehydes gave good conversion rate and selectivity. The *n*-butyric alcohol did not give excellent activity due to the steric strain. In order to examine the effects of Pb and Mg on this direct transformation of aldehydes with alcohols to corresponding esters, methacrolein and methanol were chosen as test substrates to react in the atmosphere of He and in the presence of oxygen.

Table 4 shows that the direct transformation of methacrolein with methanol in the atmosphere of He over catalysts $\text{Pd}_5/\text{Al}_2\text{O}_3$ and $\text{Pd}_5\text{Mg}_2/\text{Al}_2\text{O}_3$ had low reaction rate and selectivity. It also represented a case that neglectable rate acceleration and selectivity enhancement could be achieved by addition of Mg to catalyst $\text{Pd}_5/\text{Al}_2\text{O}_3$ in inert atmosphere. In the presence of oxygen, rate acceleration and selectivity enhancement all could be achieved over monometallic $\text{Pd}_5/\text{Al}_2\text{O}_3$ catalyst. Addition of Mg to catalyst $\text{Pd}_5/\text{Al}_2\text{O}_3$ had a positive effect for the reaction rate in the atmosphere of O_2 [31]. Addition of Pb to catalyst $\text{Pd}_5/\text{Al}_2\text{O}_3$ had a positive effect for rate acceleration and selectivity enhancement in the presence of oxygen or not, leading to high reaction rate and selectivity [28]. When Pb and Mg was doped to catalyst $\text{Pd}_5/\text{Al}_2\text{O}_3$, the reaction rate could be accelerated and selectivity also be enhanced independent of oxygen, afforded 57.7% conversion rate and 41.5% selectivity in the atmosphere of He and 93.7% conversion rate and 80.6% selectivity in the atmosphere of O_2 . The results indicated that the direct transformation of methacrolein with methanol in the presence of oxygen were faster than that in inert atmosphere.

Table 4

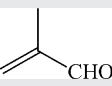
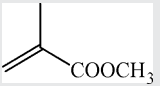
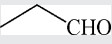

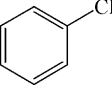
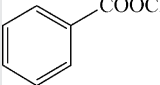
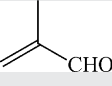
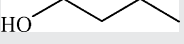
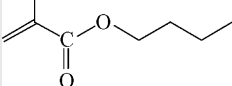
Direct transformation of methacrolein (Schemes 2 and 3) with methanol in the atmosphere of He or O_2 (for conditions see Section 2).

Entry	Catalyst	Atmosphere	Conversion rate (%)	Selectivity (%)
1	$\text{Pd}_5/\text{Al}_2\text{O}_3$	He	7.3	4.9
		O_2	34.0	42.1
2	$\text{Pd}_5\text{Mg}_2/\text{Al}_2\text{O}_3$	He	8.4	5.0
		O_2	81.5	45.1
3	$\text{Pd}_5\text{Pd}_5/\text{Al}_2\text{O}_3$	He	15.0	31.5
		O_2	65.5	68.5
4	$\text{Pd}_5\text{Pb}_5\text{Mg}_2/\text{Al}_2\text{O}_3$	He	57.7	41.5
		O_2	93.7	80.6

Preliminary studies revealed complex reaction networks typical for direct transformation of methacrolein (1) to methyl methacrylate (2) in inert atmosphere (Scheme 2) and in the presence of O_2 (Scheme 3). Catalyst compositions ($\text{Pd}_5/\text{Al}_2\text{O}_3$, $\text{Pd}_5\text{Pb}_5/\text{Al}_2\text{O}_3$, $\text{Pd}_5\text{Mg}_2/\text{Al}_2\text{O}_3$ and $\text{Pd}_5\text{Pb}_5\text{Mg}_2/\text{Al}_2\text{O}_3$) and reaction atmospheres (He and O_2) had large influences on relative contributions of various products, the overall scheme was valid for all cases.

In the atmosphere of He, besides the little target reaction of methacrolein (1) with methanol to methyl methacrylate (2) over catalysts $\text{Pd}_5/\text{Al}_2\text{O}_3$ and $\text{Pd}_5\text{Mg}_2/\text{Al}_2\text{O}_3$, major reaction was production of (3) through saturation of C=C bond with methanol (Scheme 2). For catalysts $\text{Pd}_5\text{Pb}_5/\text{Al}_2\text{O}_3$ and $\text{Pd}_5\text{Pb}_5\text{Mg}_2/\text{Al}_2\text{O}_3$, major side reactions were production of saturated aldehyde (5) and saturated ester (6) through saturation of C=C bond with hydrogen, and unsaturated alcohol (7) through saturation of C=O bond with hydrogen. Formation of by-products (5) and (6) were simply interpreted as a transfer hydrogenation reaction in which the reactant itself played the role of hydrogen acceptor. A similar reaction was the transformation of (1) to by-product (7). It showed that allylic aldehyde could act as hydrogen acceptor on the Pd surface. From analysis above, the good reaction rate and selectivity of direct transformation of methacrolein with methanol in the atmosphere of He over supported Pd_3Pb crystal catalyst indicated that the production of intermediate was not related to oxygen, and the intermediate might be hemiacetal, not methacrylic acid. The reactions over Pd_3Pb crystal catalysts slowed down in the atmosphere of He due to the partial coverage of Pd surface with co-product hydrogen and surface impurity.

Table 3
Oxidative esterification of aldehydes with alcohols to corresponding esters (for conditions see Section 2).

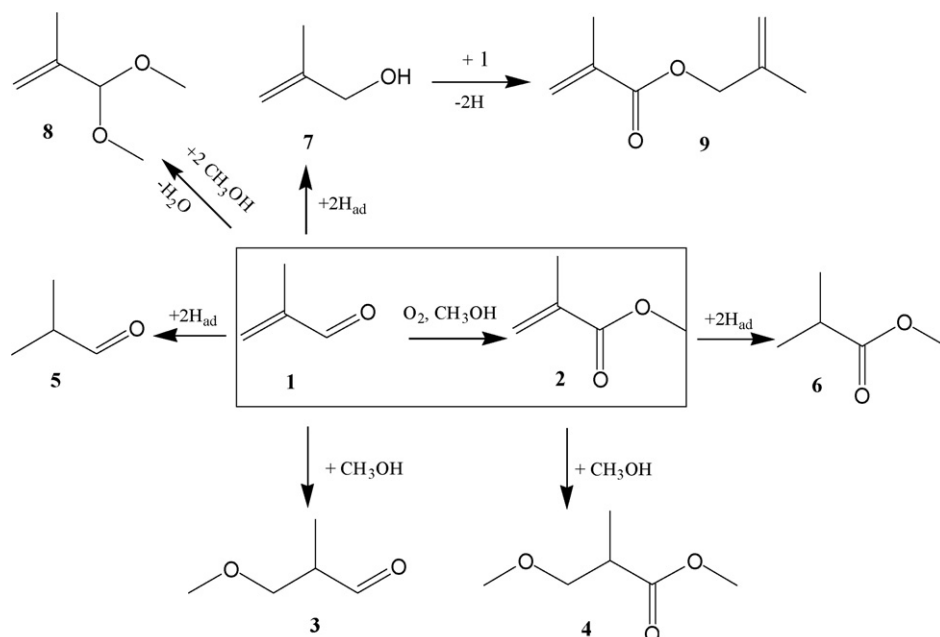
Entry	Aldehyde	Alcohol	Product	Conversion rate (%)	Selectivity (%)
1		HO-CH ₃		93.7	80.6 ^a
2		HO-CH ₃		93.2	76.8 ^b
3		HO-CH ₃		80.1	66.4 ^c
4				59.3	54.4 ^d

^a By-products detected by GC-MS were methyl formate, propylene, methyl acrylate and acetal.

^b By-products detected by GC-MS were methyl formate, propyl alcohol, propionic acid, methyl acrylate and acetal.

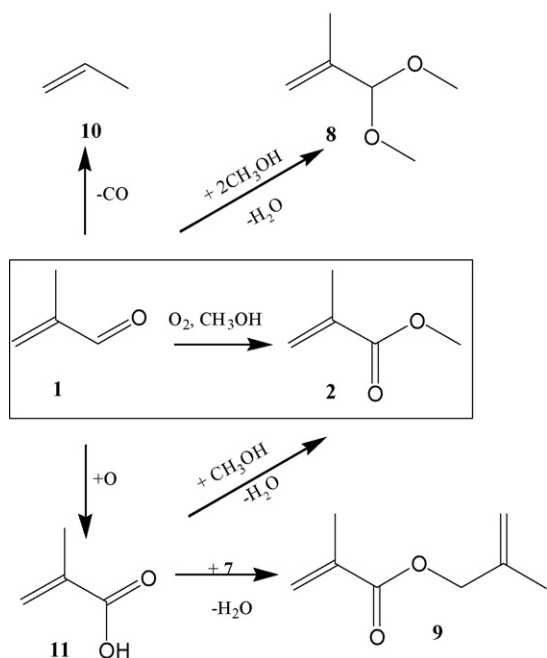
^c By-products detected by GC-MS were methyl formate, benzoic acid and acetal.

^d By-products detected by GC-MS were butyraldehyde, methacrylic acid and butyl butyrate.



Scheme 2. Reaction network in oxidative esterification of methacrolein to methyl methacrylate in the atmosphere of He.

In contrast, the presence of oxygen could suppress by-product formation of hydrogenation of both C=C bond and C=O bond. Oxygen could remove co-product hydrogen rapidly from Pd surface. A major side reaction in the atmosphere of oxygen was decarbonylation of (**1**) to by-product (**10**) (Scheme 3) [32]. Note that supported nano-Pd crystal catalyst was also good catalyst for aldehyde decarbonylation in the presence of oxygen. In order to suppress side reaction decarbonylation, the flow rate of oxygen should be controlled. Little amounts of by-products (**8**) and (**9**) were formed over doped and undoped Pd catalyst in the atmosphere of He and in the presence of oxygen [33]. There was little indication of methacrylic acid in the reaction atmosphere of O₂, and the probable reason was



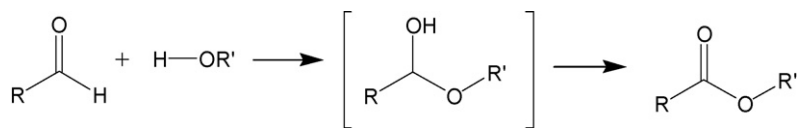
Scheme 3. Reaction network of oxidative esterification of methacrolein to methyl methacrylate in the atmosphere of O₂.

that the production of hemiacetal of aldehyde with methanol was faster than the direct oxidation of the carbonyl group.

From the analysis above, the positive effect of Mg doping in catalyst Pd₅/Al₂O₃ on direct transformation was clearly related to the presence of oxygen, and the rate acceleration was by a factor of 2.4. In the atmosphere of He, main reaction for catalysts Pd₅/Al₂O₃ and Pd₅Mg₂/Al₂O₃ was saturation of C=C bond with methanol, which indicated that monometallic Pd catalyst had neglectable effect in inert atmosphere on the main reaction of direct transformation of aldehyde with alcohol to corresponding ester. The reaction rate and selectivity in the atmosphere of O₂ over catalyst Pd₅/Al₂O₃ was higher than those in the atmosphere of He, the reason is probably that co-product hydrogen and impurity produced in surface of catalyst were removed by adsorbed chemical oxygen on surface of supported Pd catalysts to generate free active sites [32,34–36]. The positive effect of Mg doping in catalyst Pd₅/Al₂O₃ on rate acceleration in the atmosphere of O₂ might be attributed to the good adsorption and transfer of substrates methacrolein, methanol or oxygen on this catalyst.

Addition of Pb to Pd₅/Al₂O₃ enhanced the reaction rate by a factor of 2.1 in the atmosphere of He and 1.9 in the atmosphere of oxygen. Clearly, Pb accelerated reaction rate and its influence could not only be connected to the presence of oxygen. Interestingly, selectivity enhancement by addition of Pb to Pd₅/Al₂O₃ was even higher in the atmosphere of He (a factor of 7.8) than that in the atmosphere of O₂ (1.7). Obviously, the rate acceleration and selectivity enhancement was attributed to intermetallic Pd₃Pb crystals not oxygen. The factor of selectivity enhancement in the atmosphere of O₂ was lower than in the atmosphere of He, due to the over-oxidation of methacrolein to propylene and carbon dioxide in the atmosphere of O₂.

The collaborative effect of Pb and Mg doping in supported Pd catalyst on direct transformation was not related to oxygen. Reaction rate acceleration was by a factor of 7.9 in the atmosphere of He and 2.8 in the atmosphere of oxygen, and increasing selectivity was by a factor of 8.4 in the atmosphere of He and 1.9 in the atmosphere of oxygen. Interestingly, in this reaction, the rate acceleration was even higher in the atmosphere of He than that in the atmosphere of O₂. From analysis above, for all doped and undoped Pd catalysts, the selectivity in the atmosphere of oxygen was higher than that



Scheme 4. Tentative mechanism for oxidative esterification of aldehydes with alcohols to corresponding esters.

in the atmosphere of He, due to the oxidative removal of surface impurities and co-product hydrogen by oxygen adsorbed on supported Pd catalyst to impress the reaction of co-product hydrogen with substrate. Compared with the reactions in different reaction atmospheres over Pd₃Pb crystal catalysts, the factors of rate acceleration and selectivity enhancement were higher in the atmosphere of He than those in the atmosphere of O₂. This analytical result also established that the intermediate might be hemiacetal. A tentative mechanism for the direct transformation of aldehydes with alcohols to corresponding esters is proposed in Scheme 4. The reaction may proceed through the initial formation of hemiacetal intermediate, followed by oxidation of hemiacetal to generate corresponding ester.

4. Conclusions

Pb, Mg-doped Al₂O₃-supported Pd catalysts exhibited excellent activity for direct transformation of aromatic, aliphatic, and conjugated aldehydes with alcohols to corresponding esters. The positive effect of Mg doping in catalyst Pd₅/Al₂O₃ on reaction rate acceleration in the presence of oxygen was attributed to the good adsorption and transfer of substrates. On the other hand, the effect of Pb doping in catalyst Pd₅/Al₂O₃ on reaction rate acceleration and selectivity enhancement in the presence and absence of oxygen was attributed to bimetallic Pd₃Pb crystals. The collaborative effect of Pb and Mg on this Pd catalyst also increased reaction rate and selectivity independent of oxygen. For direct transformation of aldehyde with alcohol to corresponding ester over Pb, Mg-doped Al₂O₃-supported Pd catalysts in the reaction atmosphere of O₂ or He, the intermediate might be hemiacetal, not methacrylic acid. The application of Pb, Mg-doped Al₂O₃-supported Pd catalysts to other reactants and detailed reaction mechanism are currently under investigation and will be reported in due course.

Acknowledgements

The authors gratefully acknowledge the National Natural Science Funds for Distinguished Young Scholar (No. 20625618), the financial support of National Natural Science Foundation of China

(No. 20436050) and the National High Technology Research and Development Program of China (No. 2006AA06Z371).

References

- [1] E.N. Marvell, M.J. Joncich, *J. Am. Chem. Soc.* 73 (1951) 973.
- [2] E.J. Corey, N.W. Gilman, B.E. Ganem, *J. Am. Chem. Soc.* 90 (1968) 5616.
- [3] A. Abiko, J.C. Roberts, T. Takemasa, S. Masamune, *Tetrahedron Lett.* 27 (1986) 4537.
- [4] B. O'Connor, G. Just, *Tetrahedron Lett.* 28 (1987) 3235.
- [5] M. Okimoto, T. Chiba, *J. Org. Chem.* 53 (1988) 218.
- [6] R. Gopinath, A.R. Paital, B.K. Patel, *Tetrahedron Lett.* 43 (2002) 5123.
- [7] S.-I. Kiyooka, M. Ueno, E. Ishii, *Tetrahedron Lett.* 46 (2005) 4639.
- [8] H.S. Kim, T.W. Kimb, H.L. Koh, S.H. Lee, B.R. Min, *Appl. Catal. A* 280 (2005) 125.
- [9] U.R. Pillai, E. Sahle-Demessie, *Green Chem.* 6 (2004) 161.
- [10] J. Lichtenberger, D. Lee, E. Iglesia, *Phys. Chem. Chem. Phys.* 9 (2007) 4902.
- [11] R. Ubago-Peñer, F. Carrasco-Mariñ, C. Moreno-Castilla, *Catal. Today* 123 (2007) 158.
- [12] S. Carrettin, P. McMorn, P. Johnston, K. Griffin, C.J. Kiely, G.J. Hutchings, *Phys. Chem. Chem. Phys.* 5 (2003) 1329.
- [13] D.I. Enache, J.K. Edwards, P. Landon, B. Solsona-Espriu, A.F. Carley, A.A. Herzing, M. Watanabe, C.J. Kiely, D.W. Knight, G.J. Hutchings, *Science* 311 (2006) 362.
- [14] J.H.J. Kluytmans, A.P. Markusse, B.F.M. Kuster, G.B. Marin b, J.C. Schouten, *Catal. Today* 57 (2000) 143.
- [15] S. Karski, I. Witońska, *J. Mol. Catal. A* 191 (2003) 87.
- [16] S. Karski, *J. Mol. Catal. A* 253 (2006) 147.
- [17] H.H.C.M. Pinxt, B.F.M. Kuster, G.B. Marin, *Appl. Catal. A* 191 (2000) 45.
- [18] F. Alardin, H. Wullens, S. Hermans, M. Devillers, *J. Mol. Catal. A* 225 (2005) 79.
- [19] M. Comotti, C. Pina, M. Rossi, *J. Mol. Catal. A* 251 (2006) 89.
- [20] F. Alardin, B. Delmonb, P. Ruiz, M. Devillers, *Catal. Today* 61 (2000) 255.
- [21] X. Wang, R.J. Gorte, *Appl. Catal. A* 247 (2003) 157.
- [22] A.P. Markusse, B.F.M. Kuster, J.C. Schouten, *Catal. Today* 66 (2001) 191.
- [23] V.R. Gangwal, B.G.M. van Wachem, B.F.M. Kuster, J.C. Schouten, *Chem. Eng. Sci.* 57 (2002) 5051.
- [24] C. Keresszegi, J.D. Grunwaldt, T. Mallat, A. Baiker, *Chem. Commun.* (2003) 2304.
- [25] C. Keresszegi, J.D. Grunwaldt, T. Mallat, A. Baiker, *J. Catal.* 222 (2004) 268.
- [26] J.H.J. Kluytmans, A.P. Markusse, B.F.M. Kuster, G.B. Marin, J.C. Schouten, *Catal. Today* 57 (2000) 143.
- [27] T. Mallat, A. Baiker, *Catal. Today* 19 (1994) 247.
- [28] T. Miyakea, T. Asakawa, *Appl. Catal. A* 280 (2005) 47.
- [29] T.J. Lee, Y.G. Kim, *J. Catal.* 90 (1984) 279.
- [30] M.K. Oudenhuijzen, P.J. Kooyman, B. Tappel, J.A. van Bokhoven, D.C. Koningsberger, *J. Catal.* 205 (2002) 135.
- [31] W. Zhao, W.G. Cheng, Z.X. Li, L. Wang, X.P. Zhang, S.J. Zhang, *Chin. Chem. Lett.* 17 (2006) 739.
- [32] C. Keresszegi, T. Bürgi, T. Mallat, A. Baiker, *J. Catal.* 211 (2002) 244.
- [33] M.R. Crimmin, A.G.M. Barrett, M.S. Hill, P.A. Procopiou, *Org. Lett.* 9 (2007) 331.
- [34] R. DiCosimo, G.M. Whitesides, *J. Phys. Chem.* 93 (1989) 768.
- [35] T. Mallat, A. Baiker, *Catal. Today* 24 (1995) 143.
- [36] C. Keresszegi, T. Mallat, J.D. Grunwaldt, A. Baiker, *J. Catal.* 225 (2004) 138.